BOREAL ENVIRONMENT RESEARCH 14: 662–682
ISSN 1239-6095 (print) ISSN 1797-2469 (online)

Helsinki 31 August 2009

The evolution of nucleation- and Aitken-mode particle compositions in a boreal forest environment during clean and pollution-affected new-particle formation events

Petri Vaattovaara[1)]*, Tuukka Petäjä[2)], Jorma Joutsensaari[1)], Pasi Miettinen[1)], Boris Zaprudin[1)6)], Aki Kortelainen[1)], Juha Heijari[3)7)], Pasi Yli-Pirilä[3)], Pasi Aalto[2)], Doug R. Worsnop[4)] and Ari Laaksonen[1)5)]

[1)] *Department of Physics, University of Kuopio, P.O. Box 1627, FI-70211 Kuopio, Finland (*corresponding author's e-mail: petri.vaattovaara@uku.fi)*
[2)] *Department of Physics, P.O. Box 64, FI-00014 University of Helsinki, Finland*
[3)] *Department of Environmental Sciences, University of Kuopio, P.O. Box 1627, 70211 Kuopio, Finland*
[4)] *Aerodyne Research Inc., 45 Manning Road, Billerica, MA 01821-3976, USA*
[5)] *Finnish Meteorological Institute, P.O. Box 503, FI-00101 Helsinki, Finland*
[6)] *current address: Department of Physics and Astronomy, FI-20014 University of Turku, Finland*
[7)] *current address: Maritime Research Centre, Mussalontie 428, FI-48310 Kotka, Finland*

Received 15 Dec. 2008, accepted 16 Mar. 2009 (Editor in charge of this article: Veli-Matti Kerminen)

Vaattovaara, P., Petäjä, T., Joutsensaari, J., Miettinen, P., Zaprudin, B., Kortelainen, A., Heijari, J., Yli-Pirilä, P., Aalto, P., Worsnop, D. R. & Laaksonen, A. 2009: The evolution of nucleation- and Aitken-mode particle compositions in a boreal forest environment during clean and pollution-affected new-particle formation events. *Boreal Env. Res.* 14: 662–682.

We applied two tandem differential mobility analyzer methods to shed light on the evolution of the nucleation- and Aitken-mode-particle compositions at a virgin boreal-forest site during nucleation events in varying conditions. The overall results show a clear anthropogenic influence on the nucleation- and Aitken-mode-particle compositions during the events. The SO_2/MTOP and NO_x/MTOP (monoterpene oxidation products) ratios best explain the variation in the nucleation mode composition during clean and pollution-affected events, suggesting also the importance of organic sulfur compounds, in addition to other sulfur, nitrogen and organic compounds, in particle formation, composition and properties. During the cleanest events, MTOP explain well the time behaviour of the 10-nm particle composition with an estimated organic fraction of over 95%.

Introduction

The geographical extent of the tropical, temperate and boreal forests is about 30% of the Earth's land surface (e.g. Bonan 2008). Those forests are located around the world in different climate zones affecting widely atmospheric composition via new particle formation at least in European coniferous forests (e.g. Mäkelä *et al*. 1997, Kavouras *et al* 1999, Held *et al*. 2004, Vehkamäki *et al*. 2004), in European mixed coniferous and deciduous forest (Tunved *et al*. 2003), in European deciduous forest (Tunved *et al*. 2003), in European eucalypt forest (Kavouras *et al*. 1998), in European arctic hill region forest (Lihavainen *et al*. 2003), in European wetland forest (Svenningsson *et al*. 2008), in North-American coniferous forests (Marti *et al*. 1997,

Leaitch *et al*. 1999), in South-American rain forest (Rissler *et al*. 2006), in Australian Eucalypt forest (Suni *et al*. 2008), and in Asian mixed coniferous and deciduous forests (Dal Maso *et al*. 2008). Additionally, European aquatic kelp forests are known to produce a high amount of new nanometer-sized particles (e.g. O'Connor *et al*. 2008) and Asian aquatic mangrove forests (Chatterjee *et al*. 2006) and African savanna forests (Laakso *et al*. 2008) have a high potential to contribute to new particle formation.

The boreal forests solely cover one third of the forests extent and are one of the largest vegetation environments, forming a circumpolar band throughout the northern hemisphere continents, with a high potential to affect climate processes (e.g. Tunved *et al*. 2006, Spracklen *et al*. 2008, Bonan 2008). New particles are frequently formed in virgin boreal forests (e.g. Mäkelä *et al*. 1997, Kulmala *et al*. 2004, Dal Maso *et al*. 2008), and this provides an opportunity to study the properties of biogenic secondary organic aerosols (SOA) during individual nucleation events *in situ*. Boreal forests are known to emit numerous volatile and semivolatile organic gases such as various monoterpenes (e.g. Jansson *et al*. 2001, Tarvainen *et al*. 2005, Sellegri *et al*. 2006), which are oxidized in the air and form secondary organic compounds (e.g. Sellegri *et al*. 2006) which can take part in aerosol formation (e.g. O'Dowd *et al*. 2002, Laaksonen *et al*. 2008a) and growth processes in different particle sizes (e.g. Allen *et al*. 2006, Cavalli *et al*. 2006, Laaksonen *et al*. 2008a). However, in order to more fully understand the possible climatic effects of the forests, the properties of secondary organic aerosols in varying conditions (e.g. a change in meteorological parameters or in the concentrations of biogenic and antropogenic trace gases) need to be better known.

Increasing our understanding of these properties in varying conditions requires instrumental methods with high sensitivity and near-online time resolution which are suitable for the small size (diameter < 20 nm) and low mass of nucleation mode particles, the brevity of nucleation events and the rapid changes that may occur in particle composition. In this study, we applied two tandem differential mobility analyzer (TDMA) systems in parallel, namely the UFO-TDMA (ultrafine organic TDMA: Joutsensaari *et al*. 2001, Vaattovaara *et al*. 2005) and the UFH-TDMA (ultrafine hygroscopicity TDMA; Hämeri and Väkevä 2000, Petäjä *et al*. 2005) to indirectly (via physico-chemical properties) study the composition behaviour of nucleation mode particles as a function of time during boreal forest nucleation events in clean and pollution-affected conditions. The measurements were conducted at a virgin boreal forest research site, Hyytiälä, Finland, during spring 2003, which was characterized by frequent nucleation events.

Additionally, we performed simple linear regression analyses in order to investigate how the particle hygroscopic (HGF) and ethanol (EGF) growth factors, which are indirectly connected with the composition of the particles, were influenced by meteorological parameters and by gas-phase species during the nucleation events. Overall, the focus was on the reasons behind the time behaviour of newly-formed 10 nm particle compositions in varying conditions, but the links between the compositions of the different sized particles from 6 to 50 nm in diameter were also studied.

Methods

Tandem differential mobility analyzers

A tandem differential mobility analyzer (TDMA) method (Liu *et al*. 1978) provides an insight into interaction between aerosol particles and their surroundings. Briefly, the method utilizes two differential mobility analyzers (DMAs) in series. The first DMA selects a monodisperse sample from a polydisperse aerosol particle population. Then these particles are brought to a different thermodynamic environment in a controlled manner, where they can grow or shrink to a different equilibrium size in accordance with their new environment. This alteration in size is subsequently monitored with the second DMA. The ratio between the measured size in the second DMA and the size selected with the first DMA is called a growth factor (GF).

In this study, two different kinds of TDMAs were used. In a hygroscopicity TDMA (e.g.

McMurry and Stolzenburg 1989, Hämeri and Väkevä 2000) the growth of the selected particles in elevated relative humidities was monitored. On the other hand, the organic TDMA (Joutsensaari *et al.* 2001, Vaattovaara *et al.* 2005) relied on ethanol uptake by the particles. Depending on the chemical composition of the particles, different amounts of water and ethanol are consumed at a given saturation ratio by the particles. We applied the ultrafine specific versions of the TDMAs, namely the UFO-TDMA (ultrafine organic TDMA; Vaattovaara *et al.* 2005, *see* also Joutsensaari *et al.* 2001) and the UFH-TDMA (ultrafine hygroscopicity TDMA; Hämeri and Väkevä 2000) to monitor the evolution of the nucleation mode and the lower end of Aitken mode sized particles' compositions as a function of time and size in varying conditions. The dry diameters used were 6, 8, 10, 20, 30, and 50 nm for the UFO-TDMA and 8, 10, 20, 30, and 50 nm for the UFH-TDMA. The error estimate of the GF values of the consecutive UFO-TDMA measurements is smaller than 0.01 for 10–50 nm particles, 0.13 for 8 nm particles, and 0.017 for 6 nm particles (for 6 and 8 nm particles the estimation was carried out based on the 0.1 uncertainty in the particle diameter measurements, i.e. 0.1/6 and 0.1/8; Vaattovaara *et al.* 2005). For UFH-TDMA, Hämeri *et al.* (2000) estimated that the overall accuracy in determining the relative size changes with DMA is better than 1%. The saturation ratios (S, unit%) were 82%–83% for the UFO-TDMA and 90% for the UFH-TDMA.

The usefulness of the UFO-TDMA in the atmospheric background conditions has been demonstrated in laboratory measurements for 6–50 nm nanoparticles (Vaattovaara *et al.* 2005). It is due to the fact that atmospherically important ultrafine (i.e. diameter < 100 nm) inorganic particles, sodium chloride and ammonium sulfate, do not grow (i.e. EGF is 1) in the subsaturated (S = 82%–84%) ethanol vapour. On the other hand, particles composed of biogenic organic compounds (e.g. citric acid or tartaric acid) do grow (i.e. EGF is clearly over 1) at sizes between 8–50 nm. Importantly, these measurements are consistent with the bulk ethanol solubility of inorganic and organic compounds given in the literature (e.g. Lide and Frederikse 1996). For 10 nm nucleation-mode particles, EGF values are 1.12 for citric acid and 1.05 for tartaric acid at about 83% ethanol subsaturation. Furthermore, the laboratory measurements show that neither particles of pure ammonium bisulfate nor particles containing ammonium bisulfate and sulfuric acid with sulfuric acid mass fraction up to 33% grow in subsaturated ethanol vapour when the dry particle diameter is 10 nm or smaller and S < 84% (Vaattovaara *et al.* 2005). Hence, the nucleation mode particles should contain some oxidized organic material, if they grow in about 83% ethanol saturation ratio, which was also used in this study.

In the UFH-TDMA on the other hand, particles composed of inorganic salts grow typically very well. For example, at 90% relative humidity (RH) 10 nm ammonium sulfate particles exhibit hygroscopic growth factors (HGF) of 1.38 (Väkevä *et al.* 2002), whereas α-pinene and limone oxidation products, as examples of boreal forest relevant compounds, grow significantly less in chamber conditions. For example, Virkkula *et al.* (1999) measured HGFs of 1.1 for 50 nm particles at 84% RH in α-pinene and limonene oxidation experiment, Saathoff *et al.* (2003) measured HGFs of 1.10–1.11 for 100 nm and 200 nm particles at 85% RH in α-pinene oxidation experiment and Varutbangkul *et al.* (2006) measured HGFs of 1.06–1.1 for 80–100 nm particles at 85% RH in terpene photooxidation experiment. The corresponding HGF range according to Wise *et al.* (2003) is quite larger for single organic acids, varying from 1.00 (succinic and oxalic acid) to 1.51 (1-maleic acid) at 90% RH estimated from bulk properties of organic solutions.

Thus, the UFO-TDMA and the UFH-TDMA provide complementary information about the solubility of the particles to ethanol and water, which can be used to indirectly probe the composition behaviour of the particle phase. The UFH-TDMA also provides important data on the hygroscopicity of atmospheric particles (e.g. CCN, cloud condensation nuclei).

The field site and supporting field data

The nucleation event-related field measurements were carried out as a part of the EU-funded

Quantification of Aerosol Nucleation in the European Boundary Layer (QUEST) intensive field campaign at the SMEAR II (the Station for Measuring Forest Ecosystem–Atmosphere Relations) forest (61°51´N, 24°17´E, 170 m a.s.l.; for details *see* Hari and Kulmala 2005), located in Hyytiälä, upper Pirkanmaa (the province of Western Finland). The measurements were conducted during a three-week spring period (18 March 2003–8 April 2003), when the forest floor was still covered by snow. The SMEAR II is currently located in a rather homogenous over 40-year-old Scots pine (*Pinus sylvestris*) stand in which the first newly-formed ultrafine particles were observed experimentally over 10 years ago (Mäkelä *et al*. 1997). The most intensive event periods occurs during spring (Dal Maso *et al*. 2005). This campaign was characterized by frequent nucleation events (i.e. fresh 3–10 nm aerosol particles were simultaneously clearly present), accumulating a total of 15 events during the 21-day campaign.

During the QUEST field campaign in Hyytiälä, the UFO-TDMA and the UFH-TDMA systems were set up in a container situated in the central area of the SMEAR II. Inlet drew air from a height of about 4 m through 10 mm (in diameter) steel tube inside the forest canopy. A part of the UFO-TDMA and UFH-TDMA measurements of this campaign has been presented in Petäjä *et al*. (2005) and in Laaksonen *et al*. (2008a).

The facilities of SMEAR II enabled us to follow accurately the parameters describing local conditions, including trace gas concentrations (CO, NO_x, SO_2, O_3, H_2O), meteorological conditions (temperature, relative humidity, wind speed and direction) and submicron aerosol particle number size distribution starting from 3 nm in mobility diameter. Additional information about the station and its instrumentation can be found in Aalto *et al*. (2001) and in Hari and Kulmala (2005).

In addition, in this study temperature- and light-dependent emissions of monoterpenes (Tarvainen *et al*. 2005), measured concentrations of monoterpene oxidation products (MTOP; Sellegri *et al*. 2005), concentration of gaseous phase sulfuric acid (Boy *et al*. 2005) and particulate phase nitrate data (Allan *et al*. 2006) were utilized in the interpretation of the TDMA data. All the data were measured during the same Hyytiälä QUEST campaign. Furthermore, additional 10 nm and 50 nm UFO-TDMA measurements were conducted during spring 2007 in four different ethanol saturation ratios (i.e. 20%, 60%, 70%, 80%) at the same Hyytiälä site. These aid our discussion on the nature of nucleation-mode and lower end of Aitken-mode sized particles at this boreal forest environment.

Various gas phase concentrations, wind direction (WD), temperature (T) and the measured growth factors in the ethanol (EGF) and water (HGF) vapours during the Hyytiälä QUEST nucleation events were used for calculating linear correlations between one-hour averaged datasets in order to explain the composition behaviour of the particles during nucleation events in varying conditions. The linear correlations provide information on the relations between the meteorological parameters, the gas phase compounds and particulate-phase data.

Supporting chamber measurements

In order to obtain reference data and aid the organic TDMA data analysis of the boreal forest field measurements, we also carried out a smog-chamber and a plant-chamber measurements. Our smog-chamber measurements in EUPHORE (European Photoreactor; Becker 1996) chamber, Valencia, Spain, with the O-TDMA (organic tandem differential mobility analyzer; Joutsensaari *et al*. 2001; the syringe pump version) demonstrated that boreal forest relevant α-pinene oxidation products clearly grow in 20 nm size at about 84% ethanol vapour subsaturation (EGF over 1.20). A description of the experimental process of the α-pinene ozonolysis has been presented in Bonn *et al*. (2007).

The plant chamber (KCAR, Kuopio Center of Aerosol Research, laboratory, Kuopio, Finland) ozonolysis (ozone ca. 200 ppb) experiments with emissions of 2-year-old pines (*Pinus sylvestris*) in low NO_X (< 1 ppb) conditions were carried out in June 2007. The EGFs of the UFO-TDMA ranged from 1.13 up to 1.17 in the 10 nm size at 82%–83% saturation ratio. Note that this ratio is comparable with the UFO-TDMA

saturation ratio used in the measurements of this Hyytiälä campaign.

For the plant chamber experiments, two-year-old Scots pine (*Pinus sylvestris*) seedlings were obtained from the Suonenjoki Research Nursery of the Finnish Forest Research Institute (62°38´N, 27°04´E), Suonenjoki, Finland. The seedlings were individually planted in 0.5 liter plastic pots in 2:1 (vol/vol) quartz sand (diameter 0.5–1.2 mm, SP Minerals Partek, Finland) and fertilized sphagnum peat (Kekkilä PP6, Finland). The seedlings were fertilized once a week with 0.1% superex five fertilizer (Kekkilä, Finland). Before the experiments, the seedlings were grown in controlled conditions in the University of Kuopio Botanical Garden.

The plant chamber experiments were carried out in a continuous and constant flow-through chamber (*see* VanReken *et al*. 2006) made of Neflon™ FEP film type NF-0050 (Daikin Industries, Ltd., Japan). The chamber volume was about 2 m^3 (1.2 m × 1.2 m × 1.4 m) and it was held up with an aluminium frame. Plants emitting volatile organic compounds (VOC) were placed into a separate chamber from which the air was directed into a transparent reaction chamber, admitting a part of solar radiation (e.g. UV-A radiation) coming through room windows in order to participate in particle formation related processes. Air with the VOC was mixed with an airflow enriched with ozone at the inlet of the reactor. At the beginning of the trials, the VOC from the trees were introduced into the chamber about one hour before the ozone addition. Submicron aerosol particle number size distributions were measured using two instruments, a scanning and a fast mobility particle sizers (SMPS and FMPS) in order to follow the formation and growth of the particles. The number concentration during nucleation reached a maximum near 10^5 cm^{-3}. The total flow of air was 36 liters per minute (lpm) leading to a residence time of about one hour in the reactor chamber.

Results and discussion

In order to survey the evolution of newly-formed nucleation-mode particles as a function of time in varying conditions in a virgin boreal forest environment during new-particle formation events (when the simultaneous presence of both 3 nm and 10 nm newly-formed particles was clearly observable in the same mode), the growth factors of nucleation-mode particles were measured in ethanol and water vapours in subsaturated conditions at Hyytiälä during the QUEST-2003 spring campaign. A total of 15 nucleation events occurred during the three-week (18 Mar. 2003–8 Apr. 2003) campaign. Based on the SO_2 (> 0.5 ppb) and/or NO_x (> 1.5 ppb) concentrations (Table 1), 9 of the 15 events were classified as pollution-affected (21, 26 and 29 March; 1, 2, 3, 4, 7 and 8 April) and six as clean (18, 20, 23, 24, 25 and 28 March) events (*see* Table 1). This classification is in a good agreement (7 April is the only difference) with the air mass based categorization in Boy *et al*. (2005).

Effect of local conditions on the composition of nucleation-mode particles on a single event basis

The growth factors in the ethanol and water vapours were examined in different concentrations of SO_2, NO_x, sulfuric acid, and monoterpene oxidation products. The similarities and differences in wind direction and temperature during the observed new-particle formation events were also analyzed

Generally, the highest EGFs of the 10 nm particles were observed during the clean events whereas these events revealed the lowest HGFs (Fig. 1). During the pollution-affected events the nucleation mode EGFs were the lowest and at the same time the HGFs were the highest. The data clearly show that northern wind directions are associated with the low SO_2 and NO_x concentration levels (*see* Fig. 2 and Table 1).

Time evolution of the measured EGFs revealed that generally the 10 nm particles were more and more soluble in ethanol as the event progressed (Fig. 1). During three events the EGFs decreased whereas during one event the EGF remained at 1.08 throughout the event. One potential reason for the decrease in the EGFs of the 25.3 nucleation event was a very sudden wind direction change from a clean to a more polluted origin during the event. It is worth

Table 1. Minimum and maximum values measured for relevant gas phase compounds, meteorological parameters and 10 nm growth factors during 15 new-particle formation events from 18 March to 8 April 2003. Also estimated average sulfuric acid fraction in the newly formed particles (Boy *et al.* 2005) are shown. * = pollution-affected events. # = MTOP values based on the SO_2 concentrations, the 10 nm EGFs shown in this table, and on the regression equation shown of EGF 10 nm *vs.* SO_2/MTOP in Fig. 5a.

Nucleation event day and time		T (K)	WD	RH (%)	NO_x (ppb)	SO_2 (ppb)	H_2SO_4 ($10^6 cm^{-3}$)	Estimated H_2SO_4 fraction (%)	MTOP (ppt)	O_3 (ppb)	CO (ppb)	NO (ppb)	EGF 10 nm	HGF 10 nm
18 Mar. 2003	max	279.6	301	65.8	1.20	0.28	1.5	–	470	43.3	154.7	0.03	1.12	–
14:00–17:00	min	279.2	287	64.3	1.11	0.05	0.3	–	380	41.9	153.3	0.00	1.12	–
20 Mar. 2003	max	268.2	353	65.8	0.67	0.32	2.6	12.6	200	42.5	152.9	0.03	1.11	–
13:00–20:00	min	265.0	13	46.4	0.58	0.17	0.2	10.2	100	41.8	149.9	0.00	1.05	–
21 Mar. 2003*	max	271.9	225	45.6	3.14	0.86	5.2	9.1	360	42.3	167.5	0.37	1.08	1.37
13:00–17:00	min	271.2	218	36.5	2.20	0.43	1.4	8.5	200	40.5	155.3	0.08	1.08	1.31
23 Mar. 2003	max	280.8	259	64.1	1.36	0.24	2.5	–	800	44.1	156.5	0.03	–	1.34
13:00–15:00	min	280.2	241	61.0	1.17	0.11	0.9	–	700	43.6	145.8	0.00	–	1.20
24 Mar. 2003	max	280.6	306	54.4	0.82	0.19	2.2	–	430	45.0	140.5	0.02	1.14	1.20
12:00–17:00	min	279.2	290	46.1	0.69	0.05	0.1	–	400	44.6	136.7	0.00	1.13	1.23
25 Mar. 2003	max	279.0	313	45.3	0.85	0.14	2.5	7.8	450	44.6	139.7	0.03	1.14	1.20
12:00–18:00	min	277.2	257	34.8	0.72	0.02	0.2	6.1	360	42.3	138.6	0.00	1.12	1.16
26 Mar. 2003*	max	281.6	233	58.5	6.41	1.02	6.3	8.6	770	46.3	154.8	0.87	1.09	1.29
11:00–16:00	min	277.9	213	49.8	2.53	0.26	1.3	7.6	600	35.8	140.3	0.09	1.09	1.26
28 Mar. 2003	max	279.4	302	48.5	1.13	0.16	2.3	–	520	45.9	139.1	0.04	1.16	1.22
12:00–17:00	min	278.5	283	43.7	0.66	0.02	0.2	–	420	44.9	138.2	0.00	1.13	1.18
29 Mar. 2003*	max	280.0	218	46.1	2.12	0.39	2.2	4.8	300#	47.2	153.5	0.11	1.11	1.26
13:00–16:00	min	279.4	208	42.7	1.53	0.05	1.2	3.2	50#	44.2	145.9	0.05	1.10	1.21
1 Apr. 2003*	max	271.9	178	44.4	2.73	0.38	4.3	–	330#	38.2	161.2	0.30	1.11	1.24
11:00–18:00	min	269.6	167	39.5	1.14	0.12	0.5	–	100#	35.8	151.9	0.05	1.05	1.22
2 Apr. 2003*	max	272.8	149	39.3	1.90	1.26	4.5	16.9	620#	42.4	165.4	0.12	1.08	1.34
12:00—16:00	min	271.2	140	34.0	1.01	0.74	3.2	10.7	270#	39.7	154.8	0.06	1.05	1.29
3 Apr. 2003*	max	276.7	87	56.9	3.66	4.23	16.3	7.3	1890#	45.8	182.7	0.45	1.10	1.34
9:00–15:00	min	269.5	22	28.0	0.78	0.00	3.1	4.2	310#	35.2	153.0	0.04	1.06	1.25
4 Apr. 2003*	max	274.4	221	95.7	2.44	0.38	4.3	–	400#	38.3	159.2	0.18	1.10	1.29
10:00–14:00	min	272.2	183	45.0	1.52	0.23	0.1	–	220#	37.0	153.8	0.06	1.07	1.25
7 Apr. 2003*	max	272.5	39	45.1	0.72	0.59	5.5	15.0	660#	40.8	142.1	0.05	1.10	1.38
12:00–17:00	min	271.1	30	38.3	0.60	0.13	1.3	13.5	70#	36.7	139.3	0.00	1.07	1.27
8 Apr. 2003*	max	274.0	24	57.3	1.19	0.59	5.7	–	300#	34.7	170.2	0.14	1.08	1.30
12:00–14:00	min	272.4	17	56.0	0.98	0.32	5.0	–	150#	27.6	151.9	0.07	1.07	1.27

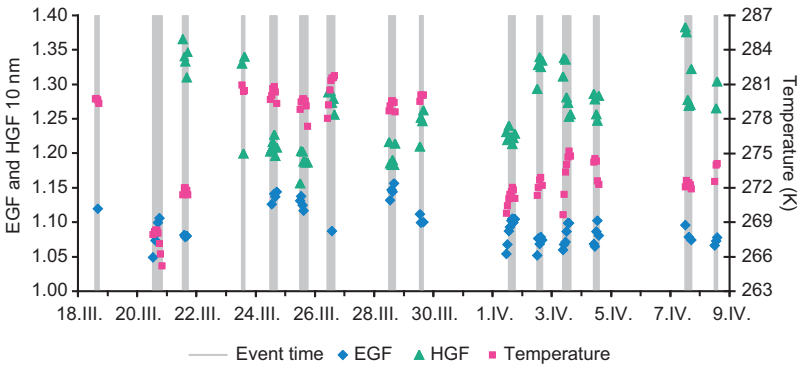

Fig. 1. The EGFs and HGFs measured for the newly-formed 10 nm particles during the new-particle formation events at Hyytiälä boreal forest site on 18 March–8 April 2003.

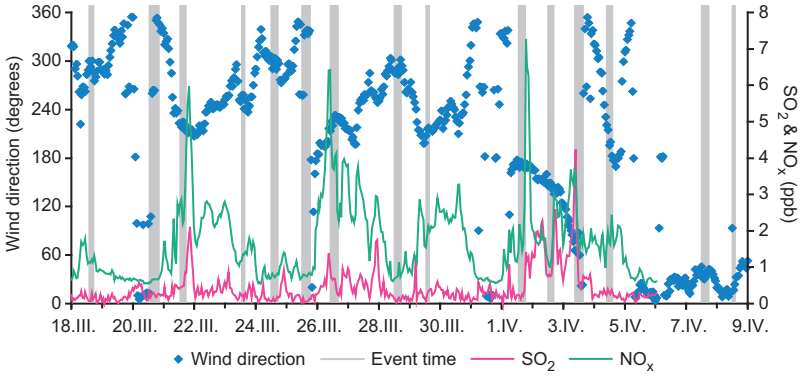

Fig. 2. Wind directions (0° and 360° stand for north), SO_2 and NO_x concentrations measured during the new-particle formation events at Hyytiälä boreal forest site on 18 March–8 April 2003.

noting that the clear presence of both 3 nm and 10 nm newly-formed particles was required in the nucleation mode at the same time, thus minimizing a time history effect on the 10 nm particles measured during the event.

During this campaign, gaseous phase sulfuric acid, an SO_2 oxidation product, had a strong diurnal cycle peaking at noon in Hyytiälä (Boy *et al*. 2005) decreasing towards the evening following the diel cycle of photochemically produced hydroxyl radical. A similar sulfuric acid cycle was also observed during spring 2007 campaign in Hyytiälä (Petäjä *et al*. 2008). During the events of the 2003 campaign (Boy *et al*. 2005), the H_2SO_4 concentrations (sulfuric acid, H_2SO_4, maximum and minimum values during individual events; *see* also Table 1) tended to decrease as the event progressed, indicating that sulfuric acid contributed less to the particle growth at later times. This suggests an explanation for the increasing trends observed in the EGFs. Even though the event of 20 March was quite clean according to the wind direction and pollution data (NO_x and SO_2 low), the measured EGFs had one of the lowest values. This could be due to differences in the monoterpene emission rates, which are temperature dependent in a boreal forest (Tarvainen *et al*. 2005). The temperatures during this event were below zero and on averaged several degrees lower than during other events. Based on this argument, during the events the ambient concentrations of monoterpenes would have been lower than during the other events. This would also lead to a low concentrations of monoterpene oxidation products during this event as observed by Sellegri *et al*. (2005; *see* Table 1). Related to that, SO_2/MTOP and NO_x/MTOP ratios (*see* Fig. 3; data of MTOP, monoterpene oxidation products, for days 18–28 March 2003) increased and the EGFs were low during the 20 March event. The higher SO_2/MTOP ratios suggest the presence of a relatively high content of sulfur containing compounds in the nucleation mode particles during this clean event. On the other hand, the higher NO_x/MTOP ratios suggest changed relative roles in monoterpene and MTOP alkyl peroxy radicals reaction pathways (i.e. there would be fewer alkyl peroxy radical self- (Eq. 1) and cross-reactions (Eq. 2) and reactions with hydroperoxy radicals (Eq. 3),

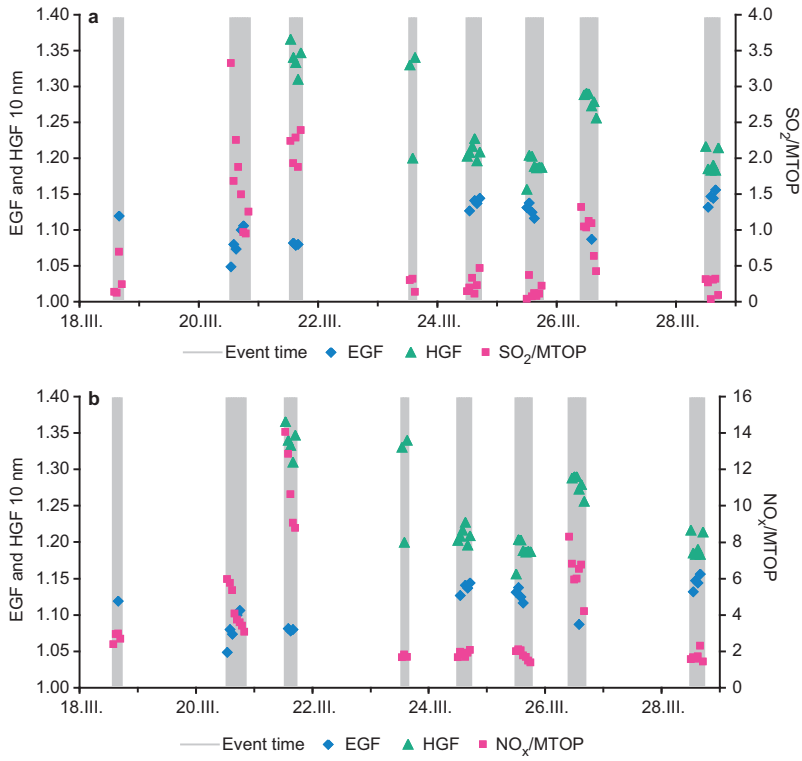

Fig. 3. EGFs, HGFs, and (**a**) SO_2/MTOP and (**b**) NO_x/MTOP ratios during the new particle formation events at Hyytiälä on 18–28 March 2003.

producing organic peroxides, and more reactions between alkyl peroxy radicals and NO (Eqs. 4a and 4b), producing alkoxy radicals and organic nitrates, than in the lower NO_x/MTOP ratio conditions.

$$RO_2 + RO_2 \rightarrow ROOR + O_2 \quad (1)$$
$$RO_2 + R'O_2 \rightarrow ROOR' + O_2 \quad (2)$$
$$RO_2 + HO_2 \rightarrow ROOH + O_2 \quad (3)$$
$$RO_2 + NO \rightarrow RO + NO_2 \quad (4a)$$
$$RO_2 + NO\ [+M] \rightarrow RONO_2\ [+M] \quad (4b)$$

Reaction in Eq. 3 may lead to formation of peroxyhemiacetals in the presence of an acid catalyst, when the peroxides react with aldehydes in the particles phase (Tobias and Ziemann 2000). Alkyl peroxy radicals may also react with NO_2 in order to produce peroxynitrates ($ROONO_2$).

Consequently, the higher NO_x/MTOP ratios make possible higher portions of organic nitrates. A recent review of the organic peroxy radical (RO_2) and alkoxy radical (RO), which can also produce variety of low-volatility compounds, chemistry with varying NO_x concentration is available in Kroll and Seinfeld (2008). Alkoxy radical path (Eq. 4a) is the major channel under conditions in which NO_x is present.

Furthermore, for alkyl peroxy radicals, reaction in Eq. 4a can form the corresponding alkoxy (RO) radical together with NO_2, or the corresponding alkyl nitrate, reaction in Eq. 4b, with the yield of the alkyl nitrate increasing with decreasing temperature (e.g. Seinfeld and Pandis 2006).

The event of 26 March is also interesting from the viewpoint of monoterpenes, because the temperature was relatively high as compared with that for low temperature events and thus the emission rates of monoterpenes and the concentrations of monoterpene oxidation products were at least comparable to those of the other events. However, the EGFs of this pollution-affected event were lower than the EGFs during the cleanest events (*see* Table 1 and Fig. 1). That is reasonable, because the SO_2/MTOP and NO_x/MTOP ratios were higher during this pollution-affected event than during the cleanest events (*see* Fig. 4). Correspondingly, the HGF values were clearly higher (*see* Table 1 and Fig. 1) during this pollution-affected event than during

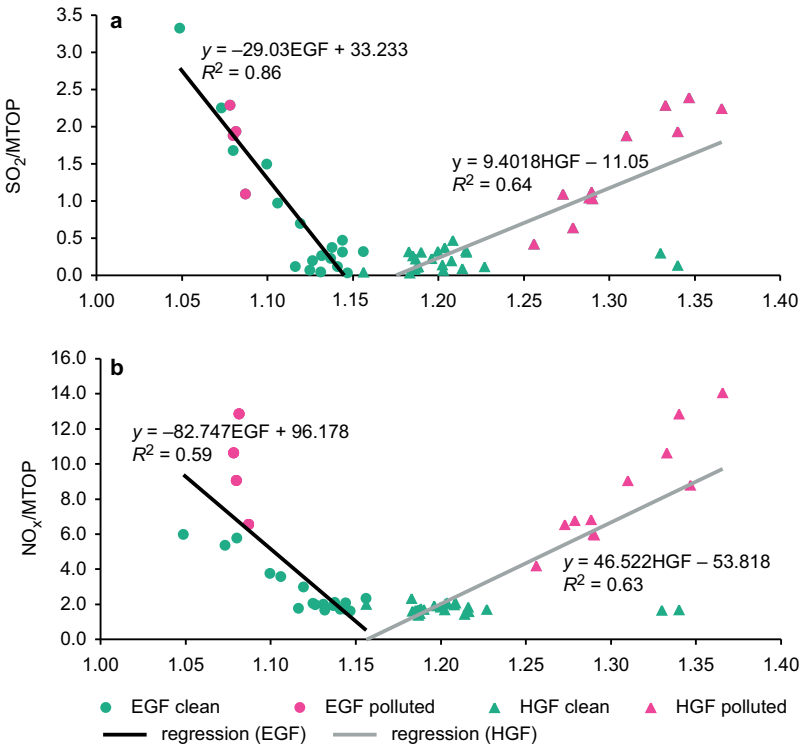

Fig. 4. (**a**) SO_2/MTOP and (**b**) NO_x/MTOP ratios compared with the EGFs and HGFs of the 10 nm particles during the new-particle formation events at Hyytiälä on 18–28 March 2003. Lines show linear regressions over all EGFs and HGFs measured for the newly-formed 10 nm particles during the nucleation events.

the cleanest events. On the other hand, the HGFs of the 26 March pollution-affected event were lower than those of the 21 March pollution-affected event. The behaviour of the HGFs can be again explained by the higher SO_2/MTOP and NO_x/MTOP ratios during the 21 March event compared to those during the 26 March event (*see* Fig. 4).

A series of four pollution-affected events from 1 to 4 April showed quite low EGFs (*see* Fig. 1). Unfortunately, MTOP concentrations were not available. Thus, we had to rely on monoterpene emission rates, temperature and NO_x concentrations for explaining the behaviour of measured growth factors. The temperature was below 0 °C during the midday 3 April event (*see* Fig. 1). According to Tarvainen *et al*. (2005) the emission rates at noon on 1 and 2 April were much lower than during the cleaner and warmer March events. On 3 April, the emission rates increased slightly but were still lower than those during March. SO_2 concentrations were low during 1 and 4 April and higher on 2 and 3 April. Consequently, sulfuric acid concentrations were also on average higher during the 2 and 3 April events than during the 1 and 4 April events. Generally, higher sulfuric acid concentrations were measured during those four pollution-affected events than during the cleanest events. This was clearly affecting the relatively high HGFs observed during this period.

To discuss further the behaviour of the EGFs of the 1, 2, 3 and 4 April pollution-affected events, let us also take a closer look at NO_x concentrations. They were similar during all of those four events and were higher than during the cleaner events. A high NO_x level chemistry produces a higher amount of relatively volatile organic nitrates and a lower amount of oxidized condensing organic compounds in α-pinene ozonolysis than a low NO_x level chemistry (*see* Presto *et al*. 2005). Because temperatures were below or close to 0 °C during the 1, 2, 3 and 4 April events, organic nitrates were most likely in particle phase during these low temperature and high NO_x level events (*see* Table 1). The NO_x/MTOP values are expected to be high due to the low temperature. The event of 21 March was a case with high NO_x/MTOP ratios and low temperature. Low temperatures make the less

oxidized relatively volatile organic compounds, as well as organic nitrates, condensable onto nucleation mode particles. Potential candidates for the formation of condensing organic nitrates are the oxidation products of sesquiterpenes (*see* Ng *et al*. 2007), and the oxidation products of monoterpenes (e.g. α-pinene). Previously, Allan *et al*. (2006) discussed the presence of organic nitrates in the accumulation mode during this same boreal forest campaign.

During the 7 and 8 April events, the temperatures were close to 0 °C and the sulfuric acid concentrations were high. Also the SO_2 and NO_x levels were above the cleanest cases. These conditions consequently lead to the low EGFs and to the high HGFs (*see* Fig. 1). The EGFs and HGFs of the 7 and 8 April events are explained similarly as the other pollution-affected events with low temperature, consequently leading to a higher SO_2/MTOP and NO_x/MTOP ratios than during the clean events.

In summary, wind direction (associated to pollution levels) and temperature are important factors to regulate the quality of air mass (biogenic *vs*. anthropogenic) which strongly affects the composition of the atmospheric newly-formed nucleation mode particles.

Relations among multiple events

In order to further study the reasons behind the composition behaviour of the boreal forest particles during the new particle formation events, we carried out a simple linear regression analyses for the EGFs and HGFs of the newly-formed 10 nm particles, with trace gas concentrations and meteorological parameters. In the following analysis, the correlation is considered very strong if $r > 0.8$, strong if $0.6 < r < 0.8$, and moderate if $0.3 < r < 0.6$. In the following, usually r^2 are shown instead of r.

Relation between the 10 nm EGFs and HGFs

The 10 nm EGF and HGF values were anticorrelated for events between 18 March and 8 April 2003 ($r^2 = 0.55$, $p = 4.2 \times 10^{-5}$, $n = 12$), and for events between 18 and 28 March 2003 ($r^2 = 0.65$, $p = 3.02 \times 10^{-8}$, $n = 44$). The anticorrelation is in agreement with the reasoning for the behaviour of the EGFs and the HGFs in varying conditions. As indicated in the earlier sections, the pollution associated with SO_2 and NO_x is an important reason for the behaviour. This is partly due to sulfur dioxide which is a precursor for sulfur-containing compounds, such as ammonium sulfate, in the particle phase. The particles of ammonium sulfate do not grow in subsaturated ethanol vapour (Vaattovaara *et al*. 2005), but are hygroscopic in the 10 nm size with the HGF of 1.38 at 90% saturation ratio (Väkevä 2002).

The effect of pine emissions on the composition of the 10 nm particles

The 10 nm particles grow, as ethanol-soluble or very-ethanol-soluble organic particles do, with the EGF values up to 1.16 at 83% saturation ratio (note that neither particles of pure ammonium bisulfate nor particles containing ammonium bisulfate and sulfuric acid with sulfuric acid mass fraction up to 33% grow in 10 nm sizes at that saturation ratio; Vaattovaara *et al*. 2005) during one of the cleanest events (28 March 2003) (Fig. 1). Importantly, the EGF of 1.16 for the newly-formed 10 nm particles during the clean event corresponds to the EGFs ranging from 1.13 up to 1.17 at 82%–83% ethanol saturation ratio observed during clean environment pine chamber ozonolysis experiment. The spring 2007 UFO-TDMA measurements with varying ethanol saturation ratios (i.e. 20%, 60%, 70%, 80%) for 10 nm particles typically showed a growth already in the lowest 20% saturation ratio and no-deliquesence type behaviour when the higher saturation ratios were applied, indicating high ethanol solubilities for nucleation mode particles, and thus a high organic content in the particles.

Monoterpene oxidation products (MTOP, data available for 18–28 March 2003, *see* Sellegri *et al*. 2005) are the natural explanation for the relatively high EGFs of nucleation mode particles in the boreal forest environment. In the previous analysis (Laaksonen *et al*. 2008a), MTOP strongly correlated with 10 nm EGFs ($r^2 = 0.64$) during this same campaign nuclea-

tion events (the presence of newly-formed 10 nm particles were required). In this study, r^2 = 0.51 ($p < 0.001$) (Table 2; the simultaneous presence of newly-formed 3 nm and 10 nm particles were required during the nucleation events), thus explaining approximately one half of the behaviour of the EGFs. When the pollution-affected events were neglected, r^2 increased to 0.84 ($p < 0.001$), thus evidently explaining composition behaviour of 10-nm particles during the clean events. The MTOP concentration was strongly correlated with temperature ($r^2 = 0.63$, $p < 0.001$) during the events. This is in agreement with the previous study by Tarvainen *et al*. (2005) who observed the relation between monoterpene emissions and temperature during this same campaign [more generally, vegetation emitted VOC are known to be dependent on the temperature and/or light (Guenther *et al*. 2006)]. However, the MTOP was not correlated with the HGFs of 10 nm event particles, but its strong correlation for the clean events was found (r^2 = 0.44; *see* Table 2; $r^2 = 0.00$ if two earlier mentioned points are ignored). These suggest also an additional contribution to the particle composition.

The role and formation of organic sulfur compounds

The commonly accepted reaction pathway for sulfuric acid (H_2SO_4) is as follows (e.g. Seinfeld and Pandis 2006):

$$OH + SO_2 \rightarrow HOSO_2 \quad (5)$$
$$HOSO_2 + O_2 \rightarrow SO_3 + HO_2 \quad (6)$$
$$SO_3 + 2H_2O \rightarrow H_2SO_4 + H_2O \quad (7)$$

During the same QUEST measurement campaign at Hyytiälä, Boy *et al*. (2005) estimated that sulfuric acid contribution to nucleation mode particle growth is on average about 9%, ranging from 3% during a clean event to 17% during a pollution-affected event (*see* Table 1). Previously, Boy *et al*. (2003) estimated the sulfuric acid contribution to be 4%–31% during autumn at the same site. During the spring 2005 cam-

Table 2. Correlation coefficients (r^2) of linear correlations between EGF 10 nm and *y*, and between HGF 10 nm and *y*. Numbers of observation pairs (*n*) are also shown. *y* = variables during 15, 8, and clean new-particle formation events when 3–10 nm newly-formed particles were clearly observable. MTOP data obtained from Sellegri *et al.* (2005; 8 events) and sulfuric acid data from Boy *et al.* (2005; 15 events). + = an increasing trend; – = a decreasing trend. r^2 in parenthesis indicate correlations or anticorrelations if two measurement points are ignored in UFH-TDMA data due to the possible effect of pre-existing nucleation mode sized particles (significance not calculated). Significance levels: * = $p < 0.05$, ** = $p < 0.01$, *** = $p < 0.001$, NS = not significant.

y	Correlation coefficient (r^2)					
	EGF 10 nm			HGF 10 nm		
	15 events (n = 55)	8 events (n = 22)	clean (n = 18)	15 events (n = 70)	8 events (n = 33)	clean (n = 22)
CO	–0.46***	–0.69***	–0.62***	+0.28*** (+0.29)	+0.70*** (+0.71)	+0.56*** (0.00)
NO_x	–0.11*	–0.14 (NS)	+0.27*	+0.15*** (+0.17)	+0.47*** (+0.21)	+0.35** (0.00)
MTOP	–	+0.51***	+0.84***	–	0.00 (NS) (–0.01)	+0.44 *** (0.00)
SO_2	–0.16**	–0.47***	–0.42**	+0.25*** (+0.28)	+0.53*** (+0.70)	+0.11 (NS) (+0.05)
WD	+0.44***	+0.49***	+0.49**	–0.32*** (–0.37)	–0.61*** (–0.64)	+0.21* (0.00)
T	+0.52***	+0.59***	+0.72***	–0.23*** (–0.30)	–0.27** (–0.41)	+0.27* (+0.15)
RH	0.00 (NS)	0.00 (NS)	–0.02 (NS)	0.00 (NS) (0.00)	0.00 (NS) (+0.03)	+0.41** (+0.09)
H_2O	+0.35***	+0.47***	+0.56***	–0.09* (–0.18)	–0.03 (NS) (–0.14)	+0.49*** (+0.14)
H_2SO_4	–0.23***	–0.31**	–0.13 (NS)	+0.35*** (+0.40)	+0.33*** (+0.43)	+0.03 (NS) (0.00)
T/SO_2	+0.26***	+0.18*	+0.11 (NS)	–0.28*** (–0.30)	–0.30*** (–0.30)	–0.12 (NS) (–0.25)
O_3	+0.36***	+0.71***	+0.64***	–0.13** (–0.16)	–0.45*** (–0.52)	+0.05 (NS) (+0.22)
SO_2/MTOP	–	–0.86***	–0.85***	–	+0.64*** (+0.88)	+0.01 (NS) (0.00)
NO_x/MTOP	–	–0.59***	–0.85***	–	+0.63*** (+0.90)	–0.02 (NS) (–0.01)
H_2SO_4/MTOP	–	–0.64***	–0.65***	–	+0.41*** (+0.57)	0.00 (NS) (0.00)

paign, Ehn *et al*. (2007a) found H_2SO_4 and 10 nm HGFs to be moderately correlated during daytime (r^2 = 0.25). In this study, during the nucleation events, r^2 for the correlation between H_2SO_4 and 10 nm EGF was 0.23 ($p < 0.001$) with a decreasing trend, and 0.35 ($p < 0.001$) for the correlation between H_2SO_4 and 10 nm HGF with an increasing trend (Table 2). The correlation coefficients (r^2) of 0.16 ($p < 0.01$) for SO_2 *vs*. 10 nm EGF with a decreasing trend, and of 0.24 ($p < 0.001$) for SO_2 *vs*. 10 nm HGF with an increasing trend during this same boreal forest spring 2003 campaign nucleation events are also in the same range ($r^2 = 0.59$, $p < 0.001$ for SO_2 correlation with H_2SO_4 during the nucleation events showing a strong correlation between sulfur dioxide and sulfuric acid concentrations). According to those linear correlations and anticorrelations (Table 2), sulfur compounds play only a minor role in the nucleation mode particle volume.

The picture changes, if the ratios of SO_2 and MTOP are used in the analysis. This finding is interesting as SO_2 is a precursor of the condensable sulfur species, such as H_2SO_4, while MTOP themselves are monoterpene oxidation products, albeit rather volatile ones. We hypothesize that SO_2 and monoterpene oxidation products participate in chemical reactions producing organosulfur compounds, such us organosulfates (e.g. Liggio and Li 2006, Ng *et al*. 2007), which then contribute to the growth of atmospheric nanoparticles.

The ratio of SO_2/MTOP was very strongly anticorrelated with the 10 nm EGFs ($r^2 = 0.86$, $p < 0.001$, Table 2), explaining very significantly the observed variance of the EGF values in varying conditions, especially during the pollution-affected nucleation events (Fig. 4a). The strong correlation between SO_2/MTOP and 10 nm HGF ($r^2 = 0.64$, $p < 0.001$) also explains the observed variance of the HGF values (Fig. 4a). The r^2 value would have even equaled 0.88 if two separate values had been ignored. Those two values were measured during the 23 March 2003 nucleation event when pollution levels were low (i.e. low sulfuric acid, NO_x and SO_2 concentrations; *see* Table 1). The hygroscopicity distribution of this event reveals that there were two kinds of particles at the start of the event: one mode corresponds with very hygroscopic particles and another mode corresponds with the hygroscopicity typically detected during the clean events of this campaign. Additionally, the event was not very intensive as compared with the other events. In the middle of the event, the more hygroscopic mode disappeared for a while, but appeared again in the end of the event. However, NO_x, SO_2 or H_2SO_4 measurements, which were carried out about 50 m from the TDMA container, did not detect any signs which would support the variation of the nucleation mode composition.

Overall, SO_2 concentrations (via reaction products) clearly affect the composition formation of those nucleation mode particles during the events. The fact that nucleation events seem to stop if gas phase sulfuric acid concentration drops to 10^5 cm^{-3} also supports the importance of sulfur compounds. Interestingly, the anticorrelation between H_2SO_4/MTOP and 10 nm EGF ($r^2 = 0.63$, $p < 0.001$) and the correlation between H_2SO_4/MTOP and 10 nm HGF ($r^2 = 0.41$, $p < 0.001$) were weaker than those between SO_2/MTOP and 10 nm EGF ($r^2 = 0.86$, $p < 0.001$) or between SO_2/MTOP and 10 nm HGF ($r^2 = 0.63$, $p < 0.001$) (Table 2). The difference can be explained using the additional $HOSO_2$ oxidation pathway

$$HOSO_2 + O_2 + M \rightarrow HOSO_2O_2 + M \quad (8)$$

(i.e. Eq. 8 in addition to Eq. 6) forming peroxy type sulfur compound radicals (*see* Berndt *et al*. 2007, 2008, Laaksonen *et al*. 2008b), which make possible the direct formation of sulfur compounds other than sulfuric acid. The formation of organosulfates from monoterpene oxidation products has been detected earlier in laboratory conditions (e.g. Liggio and Li 2006, Ng *et al*. 2007, Surratt *et al*. 2007). They proposed that organosulfates (sulfate esters) were formed from reactions of MTOP (e.g. pinonaldehyde, which belongs to MTOP) and sulfuric acid. This would explain, why anticorrelations between 10 nm EGFs and H_2SO_4/MTOP have higher r^2 values (0.64, $p < 0.001$) than between MTOP and EGF ($r^2 = 0.51$, $p < 0.001$) during the events from 18 to 28 March 2003 (Table 2). The correlation between 10 nm HGFs and H_2SO_4/MTOP was also strong ($r^2 = 0.41$, $p < 0.001$) but HGFs and MTOP were not correlated ($r^2 = 0.00$, NS).

However, the additional SO_2 reaction pathway (Eq. 8) including peroxy type sulfur compounds (Berndt *et al*. 2007, Berndt *et al*. 2008, Laaksonen *et al*. 2008b) would explain why the correlation between 10 nm GF and SO_2/MTOP is higher than that between 10 nm GF and H_2SO_4/MTOP during the events. Berndt *et al*. (2008) proposed that up to 30% of $HOSO_2$ can be converted into $HOSO_2O_2$. Because it is a peroxy-type radical and, analogous to organic peroxy radicals (RO_2), it can react with HO_2, other peroxy radicals or with NO and NO_2 (*see* e.g. Finlayson-Pitts and Pitts 2000).

This indicates tentatively an important atmospheric pathway which is also able to produce organic sulfur compounds directly without a sulfuric acid reaction. Potential products from the Eq. 6 pathway (Berndt *et al*. 2008, Laaksonen *et al*. 2008b) in NO_x free conditions include peroxy sulfuric acid (Eq. 9), organic peroxy sulfates (Eq. 10) and $HOSO_2OSO_3$ (Eq. 11).

$$HOSO_2O_2 + HO_2 \rightarrow HOSO_2O_2H + O_2 \quad (9)$$
$$HOSO_2O_2 + RO_2 \rightarrow HOSO_2OOR \quad (10)$$
$$HOSO_2O_2 + SO_2 \rightarrow HOSO_2OSO_3 \quad (11)$$

As $HOSO_2$ radical is analogous to organic peroxy radicals (RO_2), also self-reactions could be possible.

$$HOSO_2O_2 + HOSO_2O_2 \rightarrow HOSO_2OOSO_2OH \quad (12)$$

The presence of NO_x could also make sulfur nitrates possible, analogically to reactions of organic peroxy radicals. Like RO_2, $HOSO_2O_2$ would react with NO producing also organic alkoxy radical (RO) type sulfur radical

$$HOSO_2O_2 + NO \rightarrow HOSO_2O + NO_2 \quad (13)$$

or a sulfur nitrate

$$HOSO_2O_2 + NO\ [+M] \rightarrow HOSO_2ONO_2\ [+M] \quad (14)$$

Note that alkoxy radical (RO) formation is the major channel for organic peroxy radicals (RO_2) when NO_x is present. Reactions of the alkoxy-type sulfur radical, including an acidic part, could play an important role in the Eq. 6 reaction pathway chemistry.

Interestingly, the additional reaction channel in Eq. 8 makes the sulfur chemistry more complicated connecting organic chemistry, sulfur chemistry and nitrogen chemistry. Naturally, the reaction channel occurred is highly dependent on the relative amount of reactants available. For example, the correlation between 10 nm EGF and MTOP was very strong ($r^2 = 0.84$, $p < 0.001$; Table 2) during the clean events, suggesting less organosulfur compound formation during the clean (a low SO_2 gas concentration) than the pollution-affected (a higher SO_2 gas concentration) events.

Overall, based on the analysis, organic sulfur compounds seem to play an important role in the composition behaviour of the newly-formed nucleation mode particles in this boreal forest environment. Importantly, Berndt *et al*. (2008) and Laaksonen *et al*. (2008b) proposed that SO_2 oxidation products other than H_2SO_4 would be a trigger of new particle formation in atmospheric conditions.

The fraction of organic oxidation products during the clean events

The very strong correlation between MTOP and 10 nm EGF ($r^2 = 0.84$) explains well 10 nm EGFs during the clean events (Table 2). The anticorrelations between the EGFs and SO_2/MTOP or NO_x/MTOP were also very strong ($r^2 = 0.85$, $p < 0.001$ for both; Table 2), showing the importance of organic, sulfur and nitrogen chemistry during the clean events too. The highest EGFs (i.e. 1.12–1.16) of the clean Hyytiälä events (maximum particle concentration between 10^4–10^5 cm^{-3}) correspond to very-ethanol-soluble oxidation products originating from pine emission oxidation in clean plant chamber conditions (i.e. EGFs 1.13–1.17 at 82%–83% saturation ratio; maximum particle concentration slightly below 10^5 cm^{-3}). Furthermore, $r^2 = 0.64$ ($p < 0.01$) for the correlation between 10 nm EGF and O_3 (increasing trend), and $r^2 = 0.62$ ($p < 0.001$) for the correlation between 10 nm EGF and CO (decreasing trend; CO is a remarkable OH radical sink) suggest the importance of both oxidants (O_3 and OH) in the organic fraction formation during the clean events.

From the viewpoint of inorganic compounds, those EGFs are clearly higher than the EGFs observed for nucleation mode particles (with EGFs up to 1.08 for 10 nm at saturation ratio of 86%) which are known to include a high fraction of inorganic iodine oxides, in addition to a high organic fraction at the sea coast (Vaattovaara *et al*. 2006). For the Hyytiälä forest, Laaksonen *et al*. (2008a) found r^2 value of 0.965 for the correlation between particle diameter growth rates (GR, nm h^{-1}) and gas-phase MTOP concentration (ppt) during ten different nucleation events of this same spring 2003 campaign, supporting a high organic contribution to the particles. On the other hand, Boy *et al*. (2005) estimated sulfuric acid fraction in new particle formation and growth to be between 3% to 17% during the event days (Table 1). Actually, the percentage was mostly below 10%. Furthermore, Fiedler *et al*. (2005) estimated the sulfuric acid fraction to be below 10% in condensing vapours during the same campaign. Their lowest values were close to 5%. In our study, r^2 values for the correlation between GFs and H_2SO_4 were low both for 10 nm EGF (0.13, NS) and for HGF (0.03, NS) during the clean events (Table 2). Even though sulfuric acid concentrations decreased from the maximum value to the minimum value (*see* Table 1) during the event, owing to its diurnal cycle, the EGFs did not change much, which was supported by the calculated r^2 values. Overall, the organic fraction increased close to 100% at the end of the cleanest events. However, some sulfur containing acids seemed to be always present at least in small amounts [the lowest estimate (3%–4%) of Boy *et al*. (2003, 2005) may be close for sulfur compounds], the acids working also as a catalyst and pH regulator. However, the exact organic/inorganic fraction estimation is difficult, especially in the pollution-affected events, owing to $HOSO_2O_2$ radicals, sulfuric acid and their inorganic derivates which can react with different organics both in gaseous and particle phase, forming organic sulfur compounds.

According to the correlations (Table 2) and the EGFs and HGFs observed, the overall particle-phase solubility estimate of organic sulfur compounds is ethanol-insoluble or slightly-soluble and at the least slightly-water-soluble. In the cleanest events, the HGFs were still about 1.2 for 10 nm particles at 90% RH, indicating the presence of slightly-water-soluble content. Ehn *et al*. (2007a) also observed the HGFs of 1.2 at 90% RH at the same site, when the gaseous phase sulfuric acid concentration was the lowest.

The role of NO_x in the 10 nm particle composition

As introduced in earlier chapters, NO_x chemistry seems to play less important role in 10 nm particle composition in the cleanest events (i.e. a low NO_x level) than in the pollution-affected events (i.e. a higher NO_x level; *see* Fig. 4b). Consequently, various reactions of organic compounds with organic peroxy radicals, hydroperoxy radicals and each other play more dominating role in the composition formation of the 10 nm particles during the clean nucleation events than during the polluted events. Thus, the organic composition of the clean events was different than that of the pollution-affected events, because of a higher NO_x level in the pollution-affected events as compared with that in the clean events. Linear correlation shown in Fig. 4b is in agreement with this kind of chemistry. In addition to organic chemistry, NO_x may also play an important role in the sulfur chemistry (i.e. $HOSO_2O_2$ radical pathway, *see* Eqs. 13 and 14). Berndt *et al*. (2008) noticed that with increasing amounts of NO_x being present, new particle formation is inhibited. We suggest that this observation can be related to reactions given in Eqs. 13 and 14. This is because NO (nitric oxide) can react with $HOSO_2O_2$ radicals producing alkoxy radicals and nitrates, therefore decreasing the amount of $HOSO_2O_2$ reactions with HO_2, RO_2, SO_2 and itself (*see* Eqs. 9, 10, 11, and 12) and consequently decreasing also the amount of species capable of nucleating or condensing in the smallest sizes.

Similarity in the composition of 6–50 nm particles

In order to indirectly probe similarities between the nucleation-mode and the lower end of the Aitken-mode-sized particles (*see* Table 3 for

GFs), and especially the temporal evolution of their chemical compositions, we examined the correlations between the EGFs of 6–50 nm and the HGFs of 8–50 nm particles, and SO_2/MTOP and NO_x/MTOP (*see* Table 4). These linear anti-correlations with the EGFs have r^2 values of 0.30–0.86 and 0.44–0.68, respectively (*see* Table 4), and linear correlations with the HGFs have r^2

Table 3. Minimum and maximum HGFs and EGFs for 6, 8, 10, 20, 30, and 50 nm particles during 15 new-particle formation events from 18 March 2003 to 8 April 2003. * = pollution-affected events.

Nucleation event day and time		HGF				EGF					
		8 nm	10 nm	20 nm	50 nm	6 nm	8 nm	10 nm	20 nm	30 nm	50 nm
18 Mar. 2003	max	–	–	–	–	–	1.11	1.12	1.13	–	1.13
14:00–17:00	min	–	–	–	–	–	1.11	1.12	1.12	–	1.11
20 Mar. 2003	max	–	–	–	–	1.12	1.09	1.11	1.12	1.10	1.11
13:00–20:00	min	–	–	–	–	1.09	1.08	1.05	1.10	1.10	1.07
21 Mar. 2003*	max	1.29	1.37	1.43	1.48	1.09	1.08	1.08	1.09	1.12	1.14
13:00–17:00	min	1.27	1.31	1.35	1.43	1.05	1.07	1.08	1.08	1.09	1.09
23 Mar. 2003	max	1.32	1.34	1.33	1.36	–	1.08	–	1.12	1.14	1.16
13:00–15:00	min	1.21	1.20	1.29	1.21	–	1.08	–	1.12	1.14	1.16
24 Mar. 2003	max	1.33	1.23	1.25	1.32	1.11	1.14	1.14	1.18	1.21	1.19
12:00–17:00	min	1.19	1.20	1.21	1.29	1.11	1.11	1.13	1.16	1.19	1.17
25 Mar. 2003	max	1.21	1.20	1.25	1.27	1.11	1.13	1.14	1.17	1.20	1.20
12:00–18:00	min	1.14	1.16	1.19	1.19	1.09	1.09	1.12	1.15	1.17	1.18
26 Mar. 2003*	max	1.25	1.29	1.38	1.35	1.07	1.08	1.09	1.11	1.13	1.14
11:00–16:00	min	1.20	1.26	1.20	1.27	1.06	1.07	1.09	1.07	1.10	1.11
28 Mar. 2003	max	1.18	1.22	1.23	1.33	1.13	1.14	1.16	1.17	1.21	1.17
12:00–17:00	min	1.16	1.18	1.16	1.28	1.13	1.11	1.13	1.17	1.19	1.17
29 Mar. 2003*	max	1.24	1.26	1.30	1.33	1.11	1.10	1.11	1.12	1.12	1.12
13:00–16:00	min	1.19	1.21	1.20	1.26	1.09	1.08	1.10	1.10	1.10	1.09
1 Apr. 2003*	max	1.21	1.24	1.26	1.35	1.11	1.10	1.11	1.12	1.13	1.12
11:00–18:00	min	1.19	1.21	1.21	1.25	1.07	1.05	1.05	1.09	1.10	1.09
2 Apr. 2003*	max	1.32	1.34	1.40	1.51	1.09	1.07	1.08	1.11	1.10	1.14
12:00–16:00	min	1.28	1.29	1.32	1.43	1.05	1.05	1.05	1.09	1.09	1.09
3 Apr. 2003*	max	1.40	1.34	1.36	1.32	1.08	1.09	1.10	1.14	1.14	1.14
9:00–15:00	min	1.23	1.25	1.25	1.26	1.05	1.04	1.06	1.10	1.11	1.11
4 Apr. 2003*	max	1.24	1.29	1.31	1.26	1.08	1.08	1.10	1.12	1.14	1.14
10:00–14:00	min	1.19	1.25	1.21	1.19	1.07	1.05	1.07	1.10	1.11	1.10
7 Apr. 2003*	max	1.35	1.38	1.45	1.64	–	1.09	1.10	1.14	1.13	1.17
12:00–17:00	min	1.22	1.27	1.19	1.32	–	1.09	1.07	1.08	1.11	1.13
8 Apr. 2003*	max	1.24	1.30	1.34	1.40	–	1.07	1.08	1.12	1.14	1.14
12:00–14:00	min	1.23	1.27	1.24	1.35	–	1.06	1.07	1.09	1.14	1.13

Table 4. Correlation coefficients (r^2) of linear regressions between GFs of 6–50 nm particles and SO_2/MTOP and NO_x/MTOP ratios during the new-particle formation events from 18 to 28 March 2003. + = an increasing trend; – = a decreasing trend. Significance levels: * = $p < 0.05$, ** = $p < 0.01$, *** = $p < 0.001$.

GF *vs.* SO_2/MTOP	r^2: EGF (8 events; n = 17–27)	r^2: HGF (6 events; n = 33–34)	GF *vs.* NO_x/MTOP	r^2: EGF (8 events; n = 17–27)	r^2: for HGF (6 events; n = 33–34)
6 nm	–0.30*	–	6 nm	–0.51**	–
8 nm	–0.42***	+0.40***	8 nm	–0.44***	+0.36***
10 nm	–0.86***	+0.64***	10 nm	–0.59***	+0.63***
20 nm	–0.52***	+0.54***	20 nm	–0.66***	+0.48***
30 nm	–0.59***	–	30 nm	–0.68***	–
50 nm	–0.63***	+0.68***	50 nm	–0.44***	+0.56***

values of 0.40–0.68 and 0.36–0.63, respectively (*see* Table 4). This suggests that the nucleation and the lower end of Aitken-mode-sized particles have clear similarities in the composition change during the nucleation events. Laaksonen *et al*. (2008a) made a similar conclusion. In some instances, there are 10 nm particles present at the onset of nucleation which clearly belong to the old Aitken mode (*see* e.g. Petäjä *et al*. 2005: fig. 2). Thus it is possible that sometimes when the nucleation mode merges together with the old Aitken mode, 10 nm particles form an external mixture. However, in our case the events were intensive enough so that the concentrations of fresh 10 nm particles certainly overwhelmed the concentrations of aged 10 nm particles, and any influences from the old Aitken modes to the measured GFs must have been minuscule.

We also examined the relations between the EGFs and HGFs of 6–50 nm particles to study the similarity in the composition of particles during the nucleation events (Table 5). We found that the correlations between 8 nm and 10 nm, 10 nm and 20 nm (Fig. 5a), 30 nm and 50 nm, 10 nm and 30 nm, 10 nm and 50 nm (Fig. 5b), 6 nm and 10 nm (Fig. 5c), 6 nm and 8 nm, and 20 nm and 50 nm are very strong or strong (r^2 = 0.44–0.81) for the EGFs when the events from 18 March to 8 April are included in the analysis. The correlations are even stronger (r^2 = 0.54–0.89) when the analysis is restricted to the events from 18 to 28 March. For the HGFs (*see* Table 5), the correlations between 8 nm and 10 nm, 10 nm and 20 nm (Fig. 5a), 10 nm and 50 nm (Fig. 5b), and 20 nm and 50 nm are very strong or at least strong (r^2 = 0.46–0.76) when the events from 18 March to 28 March or the events from 18 March to 8 April are included in the analysis (Table 5).

It is important to note that even though the correlations suggest similarities in the composition change for the nucleation- and Aitken-mode-sized particles during the nucleation events, their overall composition is not necessarily the same because of different history of different-sized particles. The overall similarities in the particle composition can be checked comparing the absolute GFs of different-sized particles with each other during individual clean events. We notice that the values of GFs are often close to each other for different-sized particles in an oxidative environment. If the composition was the same, this should not be a case because of the Kelvin effect (*see* Vaattovaara *et al*. (2005) for the 6–50 nm particle EGF values). For example, if the 50 nm particles are very-ethanol-soluble, they should show the EGFs of about 1.45 (Vaattovaara *et al*. 2005) instead of 1.15–1.20 observed during pine chamber ozonolysis experiments and the cleanest nucleation events in the Hyytiälä forest. For 10 nm particles, the EGFs of pine chamber ozonolysis experiments, and boreal forest field measurements and very-etha-

Table 5. Correlation coefficients (r^2) of linear regressions between the GFs of 6–50 nm particles during the new-particle formation events from 18 March to 8 April 2003 (15 events) and from 18 to 28 March 2003 (eight events). The plus (+) sign indicates an increasing trend.

	Correlation coefficient (r^2)			
	EGF		HGF	
	15 events (n = 34–49)	8 events (n = 13–20)	13 events (n = 69–71)	6 events (n = 30–35)
8 *vs.*10 nm	+0.81***	+0.81***	+0.60***	+0.51***
10 *vs.* 20 nm	+0.68***	+0.77***	+0.72***	+0.76***
20 *vs.* 30 nm	+0.80***	+0.89***	–	–
30 *vs.* 50 nm	+0.73***	+0.80***	–	–
10 *vs.* 30 nm	+0.67***	+0.88***	–	–
10 *vs.* 50 nm	+0.44***	+0.68***	+0.46***	+0.50***
6 *vs.* 10 nm	+0.48**	+0.60**	–	–
6 *vs.* 8 nm	+0.45***	+0.54**	–	–
20 *vs.* 50 nm	+0.44***	+0.59***	+0.58***	+0.58***

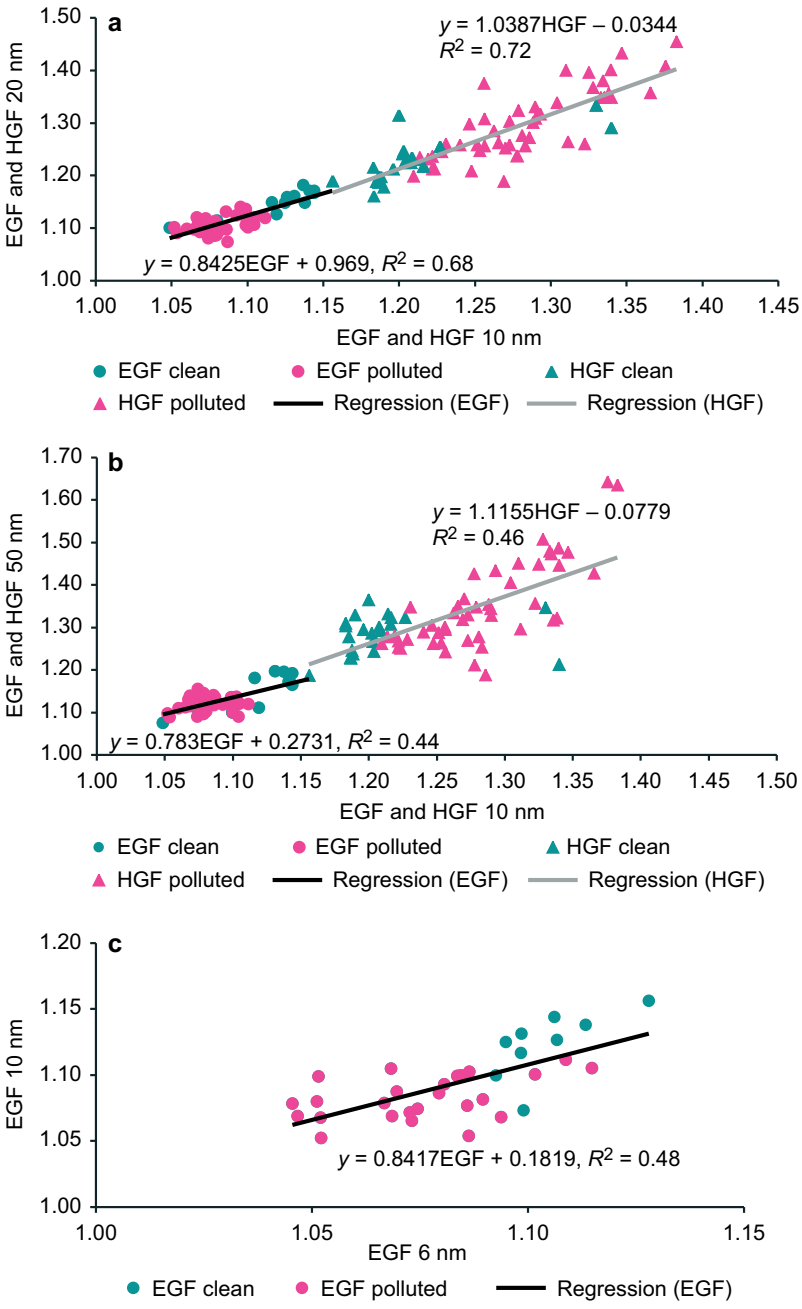

Fig. 5. (**a**) EGFs of 20 nm particles compared with EGFs of 10 nm particles, and HGFs of 20 nm particles compared with HGFs of 10 nm particles during new-particle formation events at Hyytiälä on 18 March–8 April 2003. Lines show the linear regressions over all EGFs and HGFs, measured for 20 nm and the newly-formed 10 nm particles during the nucleation events. (**b**) EGFs of 50 nm particles compared with EGFs of 10 nm particles, and HGFs of 50 nm particles compared with HGFs of 10 nm particles during new-particle formation events at Hyytiälä on 18 March–8 April 2003. Lines show the linear regressions over all EGFs and HGFs, measured for 50 nm and the newly-formed 10 nm particles during the nucleation events. (**c**) EGFs of 10 nm particles compared with EGFs of 6 nm particles during new-particle formation events at Hyytiälä on 18 March–8 April 2003. The line shows linear regression over all EGFs measured for the newly-formed 10 nm and 6 nm particles during the nucleation events.

nol-soluble organic compounds laboratory measurements, are all in good agreement with each other (i.e. EGFs around 1.13–1.16). These indicate that the overall composition of the nucleation and Aitken-mode-sized particles is not very similar in the boreal forest environment.

The dissimilarity in the composition between nucleation-mode and the Aitken-mode-sized particles may be mainly due to acid-catalyzed particle phase aging processes during the particles growth to bigger sizes, including peroxyhemiacetal formation (Tobias and Ziemann 2000), polymerization (Jang and Kamens 2001, Kalberer *et al*. 2004), hemiacetal and acetal formation, hydration and aldol condensation (Jang *et al*. 2002) and esterification (Joutsensaari *et*

al. 2004), and partly because different kinds of compounds can condense onto different sized particles depending on conditions.

In the pollution-affected cases, possible differences in the origin of different sized particles play a role too. As regards the aging process, Ehn *et al*. (2007b) observed during the Hyytiälä 2005 spring campaign that non-volatile cores of nucleation mode particles grew at an average rate of 0.6 ± 0.3 nm h^{-1} which was about a fourth of the growth rate of the particles. We suggest that the non-volatile core, observed by Ehn *et al*. (2007b), can also be related to the acid-catalyzed (e.g. sulfuric acid) aging processes listed above and the formation of organic sulfur compounds.

Conclusions

In this study, we applied the UFO-TDMA and the UFH-TDMA methods to shed light on the composition behaviour of the newly-formed nucleation (6–10 nm) and Aitken-mode (20–50 nm) sized particles within the accuracy of the methods as a function of time and size at a virgin boreal forest site, Hyytiälä, Finland, during nucleation events in varying spring conditions. Additionally, we calculated linear correlations in order to explain the variability in the growth factors observed in water and ethanol and thus the reasons behind the composition behaviour of the particles during multiple nucleation events. To aid the interpretation of the results, we utilized laboratory and plant chamber measurements, as well as the available literature.

The results show a clear anthropogenic influence on the newly-formed nucleation- and Aitken-mode sized particles composition during the events, making the particles more hygroscopic and thus increasing the capacity of Aitken-mode particles to act as cloud condensation nuclei, affecting that way the radiative balance of boreal forests. Because the emission rate of volatile organic compounds (VOCs, such as monoterpenes, for example) is temperature dependent, producing higher rates at higher temperatures, ambient temperature can regulate the atmospheric VOC concentrations in a certain temperature range. Subsequently, these have important effects on the composition and the properties of nucleation- and Aitken-mode sized particles in different vegetation zones, especially in pollution-affected cold environments such as boreal and polar regions or mountainous areas, and thus to important issues from the viewpoint of climate change.

The linear correlation analysis showed that SO_2/MTOP and NO_x/MTOP ratios well explain the event-to-event variation in the nucleation mode EGF and HGF values, and thus in the nucleation mode particles composition behaviour. The linear regression equation for the 10 nm EGF *vs*. SO_2/MTOP was also applied to estimate the concentrations of monoterpene oxidation products during the nucleation events in which MTOP were not measured. For the clean events, MTOP well explain the 10 nm particle composition behaviour with an estimate of over 95% organic fraction for the cleanest events. The difference in the particle composition and properties during the pollution-affected events compared with the clean events is a result of the different reaction pathways preferred during the varying event conditions. The results suggest that the difference is also partly due to the presence of organic sulfur and organic nitrogen compounds and a sulfate fraction, in addition to a major fraction of pure organics.

Furthermore, comparison of correlations and anticorrelations for multiple events suggest that the $HOSO_2O_2$ radical (*see* Berndt *et al*. 2007, Berndt *et al*. 2008, Laaksonen *et al*. 2008b) formation occurs in the boreal forest environment. The analysis supports the formation of organic sulfur compounds both via sulfuric acid (products such as sulfate esters) and via $HOSO_2O_2$ radical reactions (products such as organic peroxy sulfates), suggesting the importance of organic sulfur compounds, in addition to other sulfur and organic compounds, in nucleation mode particle formation, composition and properties. Importantly, NO_x play an important role both in organic and sulfur chemistry.

Even though the change in the composition is similar for 6–50 nm particles during the nucleation events, the overall composition of those particles is quite dissimilar. In unpolluted cases, this seems to be mainly due to the acid-catalyzed organic particle phase aging processes (probably including also some organic sulfur compounds),

occurring during the growth of particles in the nucleation mode and in the lower end of Aitken mode sizes. More generally, the aging processes can be expected to occur as a function of time in the particle phase.

Acknowledgements: We thank for the help provided by a large group of people during the various measurements. In particular, we wish to extend our gratitude to Vivian Paganuzzi, MA, Ville Törhönen and Jussi Kolehmainen, the staff of EUPHORE chamber and the staff of Hyytiälä field station. We are greatful for the financial support from the EU projects OSOA (Origin and fate of secondary organic aerosol), QUEST (Quantification of Aerosol Nucleation in the European Boundary Layer) and ACCENT (Atmospheric composition change the European network of excellence) and from the Finnish Academy Centre of Excellence program (project nos. 211483, 211484 and 1118615), the Emil Aaltonen Foundation, and the KCAR (Kuopio Center of Aerosol Research).

References

Aalto P., Hämeri K., Becker E., Weber R., Salm J., Mäkelä J.M., Hoell C., O'Dowd C.D., Karlsson H., Hansson H.-C., Väkevä M., Koponen I.K., Buzorius G. & Kulmala M. 2001. Physical characterization of aerosol particles during nucleation events. *Tellus* 53B: 344–358.

Allen J.D., Alfarra M.R., Bower K.N., Coe H., Jayne J.T., Worsnop D.R., Aalto P.P., Kulmala M., Hyötyläinen T., Cavalli F. & Laaksonen A. 2006. Size and composition measurements of background aerosol and new particle growth in a Finnish forest during QUEST 2 using an Aerodynyne Aerosol Mass Spectrometer. *Atmos. Chem. Phys.* 6: 315–327.

Becker K.H. (ed.) 1996. *The European photoreactor EUPHORE: Design and technical development of the European photoreactor and first experimental results*. Final report, EU project, Bruxelles.

Berndt T., Böge O. & Stratmann F. 2007. Atmospheric H_2SO_4/H_2O particle formation: mechanistic investigations. In: O'Dowd C.D. & Wagner P.E. (eds.), *Nucleation and atmospheric aerosols*, Springer, Netherlands, pp. 69–72.

Berndt T., Stratmann F., Bräsel S., Heintzenberg J., Laaksonen A. & Kulmala M. 2008. SO_2 oxidation products other than H_2SO_4 as a trigger of new particle formation. Part 1: Laboratory investigations. *Atmos. Phys. Chem.* 8: 6365–6374.

Bonan G.B. 2008. Forests and climate change: forcing, feedbacks, and the climate benefits of forests. *Science* 320: 1144–1149.

Bonn B., Korhonen H., Petäjä T., Boy M. & Kulmala M. 2007. Understanding the formation of biogenic secondary organic aerosol from α-pinene in smog chamber studies: role of organic peroxy radicals. *Atmos. Chem. Phys. Discuss.* 7: 3901–3939.

Boy M., Rannik Ü., Lehtinen K.E.J., Tarvainen V., Hakola H. & Kulmala M. 2003. Nucleation events in the continental PBL — long term statistical analyses of aerosol relevant characteristics. *J. Geophys. Res.* 108(D21), 4667, doi:10.1029/2003JD003838.

Boy M., Kulmala M., Ruuskanen T.M., Pihlatie M., Reissell A., Aalto P.P., Keronen P., Dal Maso M., Hellen H., Hakola H., Jansson R., Hanke M. & Arnold F. 2005. Sulfuric acid closure and contribution to nucleation mode particle growth. *Atmos. Chem. Phys.* 5: 863–878.

Cavalli F., Facchini M.C., Decesari S., Emblico L., Mircea M., Jensen N.R. & Fuzzi S. 2006. *Atmos. Chem. Phys.* 6: 993–1002.

Chatterjee A., Dutta C., Sen S., Ghosh K., Biswas N., Ganduly D. & Jana T.K. 2006. Formation, transformation, and removal of aerosol over a tropical mangrove forest. *J. Geophys. Res.* 111, D24302, doi:10.1029/2006JD007144.

Dal Maso M., Kulmala M. Riipinen I., Wagner R., Hussein T., Aalto P.P. & Lehtinen K.E.J. 2005. Formation and growth of fresh atmospheric aerosols: eight years of aerosol size distribution data from SMEAR II, Hyytiälä, Finland. *Boreal. Env. Res.* 10: 323–336.

Dal Maso M., Sogacheva L., Anisimov M.P., Arshinov M., Baklanov A., Belan B., Khodzher T.V., ObolkinV.A., Staroverova A., Vlasov A., Zagaynov V.A., Lushnikov A., Lyubovtseva Y.S., Riipinen I., Kerminen V.-M. & Kulmala M. 2008. Aerosol particle formation events at two Siberian stations inside the boreal forest. *Boreal Env. Res.* 13: 81–92.

Ehn M., Petäjä T., Aufmhoff H., Aalto P., Hämeri K., Arnold F., Laaksonen A. & Kulmala M. 2007a. Hygroscopic properties of ultrafine aerosol particles in the boreal forest: diurnal variation, solubility and the influence of sulfuric acid. *Atmos. Chem. Phys.* 7: 211–222.

Ehn M., Petäjä T., Birmili W., Junninen H., Aalto P. & Kulmala M. 2007b. Non-volatile residuals of newly-formed atmospheric particles in the boreal forest. *Atmos. Chem. Phys.* 7: 677–684.

Fiedler V., Dal Maso M., Boy M., Aufmhoff H., Hoffmann J., Schuck T., Birmili W., Hanke M., Uecker J., Arnold F. & Kulmala M. 2005. The contribution of sulphuric acid to atmospheric particle formation and growth: a comparison between boundary layers in northern and central Europe. *Atmos. Chem. Phys.* 5: 1773–1785.

Finlayson-Pitts B.J. & Pitts J.N.Jr. 2000. *Chemistry of the upper and lower atmosphere*. Academic Press, San Diego.

Guenther A., Karl T., Harley P., Wiedinmyer C., Palmer P.I. & Geron C. 2006. Estimates of global terrestrial isoprene emissions using MEGAN (Model of Emissions of Gases & Aerosols from Nature). *Atmos. Chem. Phys.* 6: 3181–3210.

Hämeri K. & Väkevä M. 2000. Ultrafine aerosol particle hygroscopicity and volatility in boreal forest. *Report Series in Aerosol Science* 47: 47–59.

Hämeri K., Väkevä M., Hansson H.-C. & Laaksonen A. 2000. Hygroscopic growth of ultrafine ammonium sulphate aerosol measured using an ultrafine tandem differential mobility analyzer. *J. Geophys. Res.* 105(D17):

22231–22242.

Hari P. & Kulmala M. 2005. Station for Measuring Ecosystem–Atmosphere Relations (SMEAR II). *Boreal Env. Res.* 10: 315–322.

Held A., Nowak A., Birmili W., Wiedensohler A., Forkel R. & Klemm O. 2004. Observations of particle formation and growth in a mountainous forest region in central Europe. *J. Geophys. Res.* 109, D23204, doi:101029/2004JD005346.

Jang M. & Kamens R.M. 2001. Atmospheric secondary aerosol formation by heterogeneous reactions of aldehydes in the presence of a sulfuric acid aerosol catalyst. *Environ. Sci. Technol.* 35: 4758–4766.

Jang M., Czoschke N.M., Lee S. & Kamens R.M. 2002. Heterogeneous atmospheric aerosol production by acid-catalyzed particle phase reactions. *Science* 298: 814–817.

Jansson R., Rossman K., Karlsson A. & Hansson H.-C. 2001. Biogenic emissions and gaseous precursors to forest aerosols. *Tellus* 53B: 423–440.

Joutsensaari J., Vaattovaara P., Vesterinen M., Hämeri K. & Laaksonen A. 2001. A novel tandem differential mobility analyzer with organic vapor treatment of aerosol particles. *Atmos. Chem. Phys.* 1: 51–60.

Joutsensaari J., Toivonen T., Vaattovaara P., Vesterinen M., Vepsäläinen J. & Laaksonen A. 2004. Time-resolved growth behaviour of acid aerosols in ethanol vapor with a tandem-DMA technique. *J. Aerosol Sci.* 35: 851–867.

Kalberer M., Paulsen D., Sax M., Steinbacher M., Dommen J., Prevot A.S.H., Fisseha R., Weingartner E., Frankevich V., Zenobi R. & Balternsperger U. 2004. Identification of polymers as major components of atmospheric organic aerosols. *Science* 303: 1659–1662.

Kavouras I.G., Mihalopoulos N. & Stephanou E.G. 1998. Formation of atmospheric particles from the organic acids produced by forests. *Nature* 395: 683–686.

Kavouras I.G., Mihalopoulos N. & Stephanou E.G. 1999. Formation and gas/particle partitioning of monoterpenes photo-oxidation products over forests. *Geophys. Res. Lett.* 26: 55–58.

Kroll J.H. & Seinfeld J.H. 2008. Chemistry of secondary organic aerosol: formation and evolution of low-volatility organics in the atmosphere. *Atmos. Environ.* 42: 3593–3624.

Kulmala M., Vehkamäki H., Petäjä T., Dal Maso M., Lauri A., Kerminen V.-M., Birmili W. & McMurry P.H. 2004. Formation and growth rates of ultrafine atmospheric particles: a review of observations. *J. Aerosol Sci.* 35: 143–176.

Laakso L., Laakso H., Aalto P.P., Keronen P., Petäjä T., Nieminen T., Pohja T., Siivola E., Kulmala M., Kgabi N., Molefe M., Mabaso D., Phalatse D., Pienaar K. & Kerminen V.-M. 2008. Basic characteristics of atmospheric particles, trace gases and meteorology in a relatively clean Southern African Savannah environment. *Atmos. Chem. Phys.* 8: 4823–4839.

Laaksonen A., Kulmala M., O'Dowd C.D., Joutsensaari J., Vaattovaara P., Mikkonen S., Lehtinen K.E.J., Sogacheva L., Dal Maso M., Aalto P., Petäjä T., Sogachev A., Jun Yoon Y., Lihavainen H., Nilsson D., Facchini M.C., Cavalli F., Fuzzi S., Hoffmann T., Arnold F., Hanke M., Sellegri K., Umann B., Junkermann W., Coe H., Allan J.D., Alfarra M.R., Worsnop D.R., Riekkola M.-L., Hyötyläinen T. & Viisanen Y. 2008a. The role of VOC oxidation products in continental new particle formation. *Atmos. Chem. Phys.* 7: 2657–2665.

Laaksonen A., Kulmala M., Berndt T., Sratmann F., Mikkonen S., Ruuskanen A., Lehtinen K.E.J., Dal Maso M., Aalto P., Petäjä T., Riipinen I., Sihto S.L., Janson R., Arnold F., Hanke M., Ücker J., Umann B., Sellegri K., O'Dowd C.D. & Viisanen Y. 2008b. SO_2 oxidation products other than H_2SO_4 as a trigger of new particle formation, part 2: Comparison of ambient and laboratory measurements, and atmospheric implications. *Atmos. Chem. Phys.* 8: 7255–7264.

Lide D.R. & Frederikse H.P.R. (eds.) 1996. *CRC handbook of chemistry and physics* (77th ed). CRC Press, Boca Raton, Florida.

Leaitch W.R., Bottenheim J.W., Biesenthal T.A., Li S.M., Liu S.K., Asalien K., Dryfhout-Clark H., Hopper F. & Brechtel F. 1999. A case study of gas-to-particle conversion in an eastern Canadian forest. *J. Geophys. Res.* 104: 8095–8111.

Liggio J. & Li S.-M. 2006. Organosulfate formation during the uptake of pinoaldehyde on acidic sulfate aerosols. *Geophys. Res. Lett.* 111(D24333), doi:10.1029/2005JD06978.

Lihavainen H., Kerminen V.-M., Komppula M., Hatakka J., Aaltonen V., Kulmala M. & Viisanen Y. 2003. Production of "potential" cloud condensation nuclei production associated with atmospheric new-particle formation in northern Finland. *J. Geophys. Res.* 108(D24), 4782, doi:10.1029/2003JD003887.

Liu B.Y.H., Pui D.Y.H., Whitby K.T., Kittelson D.B., Kousaka Y. & Mckenzie R.L. 1978. Aerosol mobility chromatograph — new detector for sulfuric-acid aerosols. *Atmos. Environ.* 12: 99–104.

Mäkelä J.M., Aalto P., Jokinen V., Pohja T., Nissinen A., Palmroth S., Markkanen T., Seitsonen K., Lihavainen H. & Kulmala M. 1997. Observations of ultrafine aerosol particle formation and growth in boreal forest. *Geophys. Res. Lett.* 24: 1219–1222.

McMurry P.H. & Stolzenburg M.R. 1989. On the sensitivity of particle size to relative humidity for Los Angeles aerosols. *Atmos. Environ.* 23: 497–507.

Marti J.J., Weber R.J., McMurry P.H., Eisele F.L., Tanner D.J. & Jefferson A. 1997. New particle formation at a remote continental site: assessing the contribution of SO_2 and organic precursors. *J. Geophys. Res.* 102: 6331–6339.

Ng N.L., Chabra P.S., Chan A.W.H., Surratt J.D., Kroll J.H., Kwan A.J., McCabe D.C., Wennberg P.O., Sorooshian A., Murphy S.M., Dalleska N.F., Flagan R.C. & Seinfeld J.H. 2007. Effect of NO_x level on secondary organic aerosol (SOA) formation from the photooxidation of terpenes. *Atmos. Chem. Phys.* 7: 5159–5174.

O'Connor T.C., Jennings S.G. & O'Dowd C.D. 2008. Highlights of fifty years of atmospheric aerosol research at Mace Head. *Atmos. Res.* 90: 338–355.

O'Dowd C.D., Aalto P., Hämeri K., Kulmala M. & Hoffmann T. 2002. Aerosol formation: atmospheric particles from organic vapours. *Nature* 416: 497–498.

Petäjä T., Kerminen V.-M., Hämeri K., Vaattovaara P., Joutsensaari J., Junkermann W., Laaksonen A. & Kulmala

M. 2005. Effects of SO_2 oxidation on ambient aerosol growth in water and ethanol vapours. *Atmos. Chem. Phys.* 5: 767–779.

Petäjä T., Mauldin R.L.III, Kosciuch E., McGrath J., Nieminen T., Adamov A., Kotiaho T. & Kulmala M. 2008. Measurement of sulfuric acid and OH in a boreal forest site. *Atmos. Chem. Phys. Discuss.* 8: 20193–20221.

Presto A.A., Huff Hartz K.E. & Donahue N.M. 2005. Secondary organic aerosol production from ozonolysis: 2. Effect of NO_x concentration. *Environ. Sci. Technol.* 39: 706–7054.

Rissler J., Vestin A., Swietlicki E., Fisch G., Zhou J., Artaxo P. & Andreae O. 2006. Size distribution and hygroscopic properties of aerosol particles from dry-season biomass burning in Amazonia. *Atmos. Chem. Phys.* 6: 471–491.

Saathoff H., Naumann K. H., Schnaiter M., Schock W., Mohler O., Schurath U., Weingartner E., Gysel M. & Baltensperger U. 2003. Coating of soot and $(NH_4)_2SO_4$ particles by ozonolysis products of α-pinene. *J. Aerosol Sci.* 34: 1297–1321.

Seinfeld J. & Pandis S. 2006. *Atmospheric chemistry and physics: from air pollution to climate change*. John Wiley & Sons, Inc., Hoboken, New Jersey.

Sellegri K., Hanke M., Umann B., Arnold F. & Kulmala M. 2005. Measurements of organic gases during aerosol formation events in the boreal forest atmosphere during QUEST. *Atmos. Chem. Phys.* 5: 373–384.

Spracklen D.V., Bonn B. & Carslaw K. 2008. Boreal forests, aerosols and the impacts on clouds and climate. *Phil. Trans. R. Soc. A* 366: 4613–4626.

Suni T., Kulmala M. Hirsikko A., Bergman T., Laakso L, Aalto P.P., Leuning R., Cleugh H., Zegelin S., Hughes D., van Gorsel E., Kitchen M., Vana M., Hõrrak U., Mirme S., Mirme A., Sevanto S., Twining J. & Tadros C. 2008. Formation and characteristics of ions and charged aerosol particles in a native Australian eucalypt forest. *Atmos. Chem. Phys.* 8: 129–139.

Surratt J.D., Kroll J.H., Kleindienst T.E., Edney E.O, Clayes, M., Sorooshian A., Ng N.L., Offenberg J.H., Lewandowski M., Jaoui M., Flagan R.C. & Seinfeld J.H. 2007. Evidence for organosulfates in secondary organic aerosol. *Environ. Sci. Technol.* 41: 517–527.

Svenningsson B., Arneth A., Hayward S., Holst T., Massling A., Swietlicki E., Hirsikko A., Junninen H., Riipinen I., Vana M., Dal Maso M., Hussein T. & Kulmala M. 2008. Aerosol particle formation events and analysis of high growth rates observed above a subarctic wetland-forest mosaic. *Tellus* 60B: 353–365.

Tarvainen V., Hakola H., Hellén H., Bäck J., Hari P. & Kulmala M. 2005. Temperature and light dependence of the VOC emissions of Scots pine. *Atmos. Chem. Phys.* 5: 989–998.

Tobias H.J. & Ziemann P.J. 2000. Thermal desorption mass spectrometric analysis of organic aerosol formed from reactions of 1-tetradecene and O_3 in the presence of alcohols and carboxylic acids. *Env. Sci. Tech.* 34: 2105–2115.

Tunved P., Hansson H.-C., Kerminen V.-M., Ström J., Dal Maso M., Lihavainen H., Viisanen Y., Aalto P.P., Komppula M. & Kulmala M. 2006. High natural aerosol loading over boreal forests. *Science* 312: 261–263.

Tunved P., Hansson H.-C., Kulmala M., Aalto P., Viisanen Y., Karlsson H., Kristensson A., Swietlicki E., Dal Maso M., Ström J. & Komppula M. 2003. One year boundary layer aerosol size distribution data from five nordic background stations. *Atmos. Chem. Phys.* 3: 2183–2205.

Vaattovaara P., Räsänen M., Kühn T., Joutsensaari J. & Laaksonen A. 2005. A method for detecting presence of organic fraction in nucleation mode sized particles. *Atmos. Chem. Phys.* 5: 3277–3287.

Vaattovaara P., Huttunen P.E., Yoon Y.J., Joutsensaari J., Lehtinen K.E.J., O'Dowd C.D. & Laaksonen A. 2006. The composition of nucleation and Aitken mode particles during coastal nucleation events: evidence for marine secondary organic contribution. *Atmos. Chem. Phys.* 6: 4601–4616.

Väkevä M. 2002. Studies of hygroscopic properties of nucleation mode aerosol particles. *Report Series in Aerosol Science* 55: 1–29.

VanReken T.M., Greenberg J.P., Harley P.C., Guenther A.B. & Smith J.N. 2006. Direct measurement of particles formation and growth from the oxidation of biogenic emissions. *Atmos. Chem. Phys.* 6: 4403–4413.

Varutbangkul V., Brechtel F.J., Bahreini R., Ng N.L., Keywood M.D., Kroll J.H., Flagan R.C., Seinfeld J.H., Lee A. & Goldstein A.H. 2006. Hygroscopicity of secondary organic aerosols formed by oxidation of cycloalkenes, monoterpenes, sesquiterpenes, and related compounds. *Atmos. Chem. Phys.* 6: 2367–2388.

Vehkamäki H., Dal Maso M., Hussein T., Flanagan R, Hyvärinen A., Lauros J., Merikanto J., Mönkkönen P., Pihlatie M., Salminen K., Sogacheva L., Thum T., Ruuskanen T., Keronen P., Aalto P.P., Hari P., Lehtinen K.E.J., Rannik Ü. & Kulmala M. 2004. Atmospheric particle formation events at Värriö measurement station in Finnish Lapland 1998–2002. *Atmos. Chem. Phys.* 4: 2015–2023.

Virkkula A., van Dingenen R., Raes F. & Hjorth J. 1999. Hygroscopic properties of aerosol formed by oxidation of limone, α-pinene and β-pinene. *J. Geophys. Res.* 104: 3569–3579.

Wise M.E., Surratt J.D., Curtis D.B., Shilling J.E. & Tolbert M.A. 2003. Hygroscopic growth of ammonium sulphate/dicarboxylic acids. *J. Geophys. Res.* 108(D20), 4638, doi:10.1029/2003JD003775.